

University of Nebraska - Lincoln

DigitalCommons@University of Nebraska - Lincoln

Faculty Publications from The Water Center

Water Center, The

4-15-2021

Removal of Carbamazepine onto Modified Zeolitic Tuff in Different Water Matrices: Batch and Continuous Flow Experiments

Othman A. Al-Mashaqbeh

Diya A. Alsafadi

Layal Z. Alsalhi

Shannon L. Bartelt-Hunt

Daniel D. Snow

Follow this and additional works at: <https://digitalcommons.unl.edu/watercenterpubs>





Part of the [Environmental Indicators and Impact Assessment Commons](#), [Fresh Water Studies Commons](#), [Hydraulic Engineering Commons](#), [Hydrology Commons](#), [Sustainability Commons](#), and the [Water Resource Management Commons](#)

This Article is brought to you for free and open access by the Water Center, The at DigitalCommons@University of Nebraska - Lincoln. It has been accepted for inclusion in Faculty Publications from The Water Center by an authorized administrator of DigitalCommons@University of Nebraska - Lincoln.

Article

Removal of Carbamazepine onto Modified Zeolitic Tuff in Different Water Matrices: Batch and Continuous Flow Experiments

Othman A. Al-Mashaqbeh ^{1,*}, Diya A. Alsafadi ², Layal Z. Alsalhi ¹, Shannon L. Bartelt-Hunt ³ and Daniel D. Snow ⁴

¹ Emerging Pollutants Research Unit, Royal Scientific Society, Amman 11941, Jordan; leial.salhi@rss.jo

² Biocatalysis and Biosynthesis Research Unit, Royal Scientific Society, Amman 11941, Jordan; DiyaAlhaq.Alsafadi@rss.jo

³ College of Engineering, University of Nebraska–Lincoln, Omaha, NE 68583, USA; sbartelt@unl.edu

⁴ Water Sciences Laboratory, University of Nebraska, Lincoln, NE 68583, USA; dsnow1@unl.edu

* Correspondence: othman.mashaqbeh@rss.jo

Abstract: Carbamazepine (CBZ) is the most frequently detected pharmaceutical residues in aquatic environments effluent by wastewater treatment plants. Batch and column experiments were conducted to evaluate the removal of CBZ from ultra-pure water and wastewater treatment plant (WWTP) effluent using raw zeolitic tuff (RZT) and surfactant modified zeolite (SMZ). Point zero net charge (pHpzc), X-ray diffraction (XRD), X-ray fluorescence (XRF), and Fourier Transform Infrared (FTIR) were investigated for adsorbents to evaluate the physiochemical changes resulted from the modification process using Hexadecyltrimethylammonium bromide (HDTMA-Br). XRD and FTIR showed that the surfactant modification of RZT has created an amorphous surface with new alkyl groups on the surface. The pHpzc was determined to be approximately 7.9 for RZT and SMZ. The results indicated that the CBZ uptake by SMZ is higher than RZT in all sorption tests (>8 fold). Batch results showed that the sorption capacity of RZT and SMZ in WWTP effluent (0.029 and 0.25 mg/g) is higher than RZT and SMZ (0.018 and 0.14 mg/g) in ultrapure water (1.6–1.8 fold). Batch tests showed that the equilibrium time of CBZ removal in the WWTP matrix (47 h) is much longer than CBZ removal in ultrapure water. The sorption capacity of RZT & SMZ in WWTP effluent (0.03, 0.33 mg/g) is higher than RZT and SMZ (0.02 and 0.17 mg/g) in ultrapure water (1.5–2 fold) using column test. This study has clearly demonstrated that the performance of RZT and SMZ is more efficient for the removal of CBZ from realistic wastewater than ultrapure water. It is evident that the surfactant modification of RZT has enhanced the CBZ removal in both matrices.

Keywords: carbamazepine; matrix effect; sorption; surfactant-modification; zeolitic tuff



Citation: Al-Mashaqbeh, O.A.; Alsafadi, D.A.; Alsalhi, L.Z.; Bartelt-Hunt, S.L.; Snow, D.D. Removal of Carbamazepine onto Modified Zeolitic Tuff in Different Water Matrices: Batch and Continuous Flow Experiments. *Water* **2021**, *13*, 1084. <https://doi.org/10.3390/w13081084>

Academic Editor: Juan Carlos Leyva Diaz

Received: 12 March 2021

Accepted: 5 April 2021

Published: 15 April 2021

Publisher's Note: MDPI stays neutral with regard to jurisdictional claims in published maps and institutional affiliations.



Copyright: © 2021 by the authors. Licensee MDPI, Basel, Switzerland. This article is an open access article distributed under the terms and conditions of the Creative Commons Attribution (CC BY) license (<https://creativecommons.org/licenses/by/4.0/>).

1. Introduction

Emerging pollutants such as pharmaceuticals and personal care products (PPCPs) have been detected in municipal raw wastewater entering treatment plants (influent and effluent) ranging from sub-ng/L to µg/L levels. Among these PPCPs, carbamazepine (CBZ) is the most frequently detected pharmaceutical residue in aquatic environments [1–6].

CBZ is one of the most common psychoactive drugs used for treating many human diseases such as epileptic seizures, bipolar depression, and mania [7]. CBZ has high stability, low adsorption capacity, therefore, it is poorly removed from wastewater treatment systems. Thus, CBZ is currently used as a marker to evaluate the contamination of water bodies from PPCPs [8]. Many studies have detected CBZ in raw sewage (6.3 µg/L), in wastewater treatment plants (17.3–22 µg/L), in river system (1.283 µg/L), and drinking water (0.25 µg/L) [8,9]. Exposure to CBZ through drinking water may trigger autism spectrum disorders during pregnancy [4]. Consequently, the removal of CBZ from the aqua ecosystem is recently considered a priority for many researchers.

Adsorption is widely employed to remove emerging pollutants in wastewater treatment. It is the most efficient method in terms of simplicity, the cost of design and operation, and insensitivity of toxic substances [10,11]. Several adsorbents have been developed and tested to remove CBZ from wastewater matrices (i.e., zeolite) [12,13]. Natural zeolite has potential as a sorbent in multiple applications for water treatment and purification processes due to its physico-chemical characteristics, low cost, and widespread availability [14]. It includes minerals such as clinoptilolite, mordenite, phillipsite, and chabazite which can be utilized to sorb a variety of organic and inorganic compounds [14]. However, the direct use of zeolite is often limited due to its low affinity for organic pollutants resulted from the net negative surface charge and hydrophilic surface properties [15,16]. Therefore, cost-effective surface modifications are needed to improve the sorbent capacity of zeolite materials. Studies found that zeolite can be modified with different cationic surfactants (i.e., Hexadecyltrimethylammonium bromide-HDTMA-Br) creating a hydrophobic surface that enhances the organic sorption capacity from wastewater under different experimental conditions [17–21]. Previous studies have shown that SMZ has a promising removal toward PPCPs in many applications [20,22,23]. For example, natural and modified zeolite by HDTMA-Br (SMZ) has shown significant sorption of diclofenac under different conditions [22]. While CBZ removal by SMZ has been studied using spiked CBZ in ultrapure water and/or synthetic wastewater, there is little work on the CBZ removal from realistic wastewater matrix [23]. The presence of dissolved organic matter (DOM) in secondary treated wastewater is recognized as the main factor limiting the adsorption of organic micropollutants onto activated carbon and its impact on the organic micropollutants adsorption is still unclear [23–27]. Therefore, this knowledge is needed for the design and optimization of using SMZ in the removal of PPCPs from realistic wastewater treatment systems.

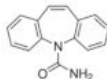
This work aims to evaluate the capacity and performance of RZT and surfactant modified zeolite by HDTMA-Br in the removal of CBZ compound from ultra-pure water and realistic wastewater (effluent). The sorption performance was further investigated under dynamic conditions using column studies under the same matrices. Furthermore, the point of zero charge, X-ray diffraction, X-ray fluorescence, and the Fourier transform infrared were performed to RZT and SMZ to understand the CBZ uptake mechanism.

2. Materials and Methods

2.1. Chemicals

Analytical-grade of carbamazepine (CBZ) and Hexadecyltrimethylammonium Bromide (HDTMA-Br) (Sigma-Aldrich Chemical Company, St. Louis, MO, USA, 99%) were used. Influent solutions comprised ~10 mg/L of CBZ while the HDTMA-Br solution was ~48 g/L. The physical properties of CBZ are shown in Table 1.

Table 1. Classification and physical and chemical properties of carbamazepine.

Compound	Chemical Structure	Drug Designation	pKa	Log Kow	Water Solubilitymg/L	Molecular Weightg/mol
Carbamazepine		Anticonvulsant	13.9	2.45	17.7	236.3

2.2. Zeolitic Tuff Preparation and Characterization

Raw zeolitic tuff was collected by the Jordanian Scientific Company for Technological Development (TechDev Co., Amman, Jordan) from the Al-Safawi area/Al-Mafraq located north-east of Jordan. These samples are referred to as raw zeolitic tuff (RZT). RZT was subjected to crushing and sieving, one size was selected for further investigation. The selected size was between 2.36 mm < selected size < 4.75 mm. The selected RZT was washed with ultrapure water (Milli-Q Ultrapure, MilliporeSigma, Molsheim, France) water

over sieve no.12 to clean it from the fine particles, then it was soaked in ultrapure water for three days. The washed RZT was manually separated from grit limestone and the percentage of removed limestone was ~4.1%. RZT was then dried at 60 °C for three days and stored for further use.

2.2.1. Surfactant Chemical Modification

Modification of the RZT surface was performed in this study using HDTMA-Br at a concentration equal to 200% of the external cation exchange capacity (ECEC) of the zeolite. The experimental ECEC value (0.144 mEq/g) was evaluated using the method suggested by de Gennaro et al., 2014 [18]. The solution equivalent was prepared by mixing 48 g of HDTMA-Br and 1000 mL ultrapure water using a magnetic stirrer at 500 rpm at 50 °C (temp. of solution) until a clear solution was reached. Then, 500 g of RZT was placed in the HDTMA-Br solution and mixed using an orbital shaker for 6-h at 120 rpm and 50 °C. The pH and EC of solution before and after were 5.674 and 2.65 mS/cm, and 8.173 and 4.9 mS/cm, respectively. After 6-h the modified RZT was washed with ultrapure water to remove the unnecessary surfactant and then dried in an oven at 35 °C for 24-h. Modified raw zeolitic tuff was referred to as surfactant modified zeolite (SMZ).

2.2.2. Point of Zero Net Charge (pzc)

pH_{pzc} of RZT and SMZ were determined according to the method described by Kragović et al., 2019 [28]. 0.1 g of crushed RZT and SMZ were transferred to six beakers (50 mL) containing 30 mL of 0.1 mol /L KNO_3 prepared in ultrapure water with adjusted pH values from 2 to 12 (pH = 2, 4, 6, 8, 10, and 12). The beakers were covered with aluminum foil and placed on the magnetic stirrer for 24-h at 500 rpm. The aqueous content of the beakers were filtered and pH was measured. The pH_{pzc} of the RZT and SMZ samples were determined as the plateau of the curve.

2.2.3. X-ray Diffraction (XRD)

Powder X-ray diffraction (XRD) patterns of the RZT and SMZ samples were recorded by XRD (Model 6000, Shimadzu Co., Kyoto, Japan) using copper $\text{K}\alpha$ irradiation ($\lambda = 1.5406$ nm) produced at 40 kV and 30 mA. The XRD diffraction patterns were obtained in the 2θ range of 5–80° at a scan speed of 3° min^{-1} .

2.2.4. X-ray Fluorescence (XRF)

The chemical compositions of the RZT and SMZ were determined using a sequential X-ray fluorescence (XRF) spectrometer (XRF-S8, Bruker Co., Tiger, Germany).

2.2.5. Fourier-Transform Infrared Spectroscopy (FTIR)

The Fourier-transform infrared (FTIR) spectroscopic measurements were carried out using an FTIR device (Prestige-21, Shimadzu Co., Kyoto, Japan) to identify functional groups on the RZT surface before and after modification (SMZ). The spectra were recorded in the range between 400 and 4000 cm^{-1} at a resolution of 4 cm^{-1} , at room temperature with a standard detector by averaging 10 scans.

2.3. Water Matrix

Two types of waters were tested throughout this study: Ultrapure water and WWTP effluent. The ultrapure water was obtained from a Milli-Q purifier (pH 7.242, EC 0.055 $\mu\text{S}/\text{cm}$, TOC 2 ppb). WWTP effluent was obtained from the discharge of the As-Samra Wastewater treatment plant at Jordan (before chlorination). The properties of wastewater samples used in this work are; Chemical Oxygen Demand (38.24 mg/L), Biological Oxygen Demand (4.26 mg/L), Total Organic Carbon (12 mg/L), Total Suspended Solids, (7.51 mg/L), Total Nitrogen, (15.68 mg/L), Total Phosphorus, (6.02 mg/L). The collected wastewater samples were stored at 4 °C until analysis and used within 3 days of collection. Both solutions were used without pH adjustment and filtration. The pH and EC values of spiked CBZ solutions

were 6.9–7.2 and 1.6–3.5 $\mu\text{S}/\text{cm}$ (Ultrapure) and 7.8–8.2 and 1779–1850 $\mu\text{S}/\text{cm}$ (WWTP effluent), respectively.

2.4. Kinetic Adsorption Experiments

A 10 mg L⁻¹ stock solution of CBZ was prepared by dissolving 50 mg CBZ in 15 mL methanol, diluted to 5 L ultrapure water, and stored at 4 °C. Batch experiments utilized 48 g of RZT and 10 g of SMZ added to 0.4 L of 10 mg/L CBZ solution in 0.5 L Erlenmeyer flask and placed on an orbital shaker (GFL/Model 3032) at 180 rpm for 36–78 h. Samples were withdrawn using a syringe at predetermined time intervals and filtered using a syringe filter 0.45 μm (25 mm Nylon welded) before analysis. All collected samples were stored at 4 °C in a refrigerator and analyzed for pH, EC, and CBZ contents. All the sorption experiments were performed without adding a buffer solution to avoid the presence of other electrolytes in the system at 20 \pm 1 °C. All the experiments were carried out in triplicate and the results were reported as means and standard deviations.

CBZ uptake at different times, q_t (mg/g) was calculated using the mass balance between the solid and the solution as follows:

$$q_t = (C_o - C_t) V/M \quad (1)$$

where q_t the amount of CBZ sorbed at time t (mg/g), C_o the initial liquid phase CBZ concentration (mg/L), C_t is the liquid phase CBZ concentration at time t (mg/L), V the initial solution volume (L) and M is the mass of mixed sorbent (g).

The pH dependence of the adsorption was also investigated in batch mode, using a fixed initial CBZ concentration of 10 mg/L and varying the pH from 2.5 to 9.5. This range of pH values was chosen based on the pKa value for the CBZ studied (Table 1). The pH of the adsorption medium was varied from 2.0 to 10.0 using the different buffer solutions prepared with ultrapure water as follows: HCl–KCl (pH 2.0), citric acid–sodium hydroxide (pH 5.0), Tris (hydroxymethyl) aminomethane sodium chloride–HCl (pH 7.0), Glycine–KOH (pH 8.0, 9.0, and 10). The pH was measured with a pH meter (Multi 9630 IDS WTW/Weilheim, Germany).

2.5. Column Adsorption Experiments

CBZ transport and treatment under continuous flow conditions were investigated in RZT and SMZ-packed columns. The experiments used a PVC class 18 column with an inner diameter of 4 cm and a length of 30 cm. The inlet and outlet tips of the threaded Teflon end-caps were fitted with stainless-steel threaded adapter Male 1/2 \times 3/16 to direct flow and take samples. The total mass of RZT and SMZ packed in the column were 88 g mixed with 530 g glass beads (74% between 0.3–0.6 mm). The column packing was carried out using a procedure outlined by Reynolds and Richards, 1996 [29]. The inlet and outlet PVC tubes were wrapped in aluminum foil to prevent photocatalytic reactions. Ultrapure water at pH 7.6 was used to condition the column for about 65-h by pumping the solution through the column upward at a flow rate range, 4.5–4.7 mL/min using a two-channel Multichannel peristaltic pump (Masterflex Model L/S[®] Precision variable-speed pump system 07528-30, Vernon Hills, IL, USA). Flushing continued until the effluent reached an EC value of 59.6 $\mu\text{S}/\text{cm}$ for the RZT column and 75.5 $\mu\text{S}/\text{cm}$ for the SMZ column. Subsequently, ultrapure water and WWTP effluent were pumped into the column from the bottom at the same flow rate (average flow rate 4.7 mL/min).

Samples of column influent and effluent were collected manually at different time intervals in 40 mL glass bottles. The collected sample was filtered using a syringe filter 0.45 μm (25 mm Nylon welded) and transferred to 2 mL vials.

The CBZ breakthrough curve for a column is determined by plotting the ratio of effluent CBZ concentration (C) to inlet CBZ concentration (C_0) against effluent volume. The maximum sorption capacity of CBZ onto RZT and SMZ in the columns was estimated using “Simpson’s Rule” based on the mass calculated from the area over the curve divided by the mass of RZT and SMZ (88 g) in the column.

2.6. Sample Analysis

pH, EC, and CBZ were measured for all samples. Concentrations of CBZ were determined using two methods; (1) Ultraviolet-visible spectroscopy (UV-VIS) (Biochrom, Libra S50) at wavelength 284 nm, and (2) with an Agilent model 1100 series High-Performance Liquid Chromatography (HPLC) equipped with a diode-array detector at 254 nm. An Agilent LiChrospher Column RP-18 (5 μm) with isocratic separation using a mixture of acetonitrile and ultrapure water ($v:v = 30:70$) at a flow rate of 1 mL/min. The sample injection volume was 10 μL and the column temperature was maintained at 25 $^{\circ}\text{C}$. A calibration curve was prepared from 10 mg/L CBZ stock solution using five calibration points (1 mg/L, 3 mg/L, 5 mg/L, 7 mg/L, 10 mg/L) for both HPLC and UV-Vis analysis. Although CBZ concentration of up to 1.5 $\mu\text{g/L}$ was reported for wastewaters [6]. The main reason for using such high CBZ concentration in the experiments was to minimize the experimental duration for removal experiments and the high detection limit of CBZ analysis (UV-vis and HPLC). Moreover, there are many compounds (organic and inorganic) in WWTP effluent which may cause interference in measuring the CBZ by UV-VIS for WWTP effluent samples. Therefore, to eliminate the matrix effect of these compounds, two calibration standard curves were prepared using the WWTP effluent and ultrapure water matrix to determine the content of CBZ in WWTP effluent and ultrapure water samples.

3. Results

3.1. Point of Zero Charge

The pH of the solution at which the charge of the positive surface sites is equal to the charge of the negative ones (i.e., the adsorbent surface charge has zero value) is considered the point of zero charge (pH_{pzc}). pH_{pzc} of adsorbent is important because it indicates the net surface charge. The surface charge is negative at $\text{pH} > \text{pH}_{\text{pzc}}$ and positive at $\text{pH} < \text{pH}_{\text{pzc}}$ [30]. The results of pH_{pzc} for RZT and SMZ are shown in Figure 1. At first, increasing in the initial pH (pH_i) from 2 to 6.0 for RZT and SMZ has caused an increase in the final pH (pH_f). After this stage, the increase in the initial pH (pH_i) from 6.0 to 8.0 has slightly caused an increase in the pH_f . When the initial pH increased from 8.0 to 10.0, it does not influence the pH_f and curves reached plateaus.

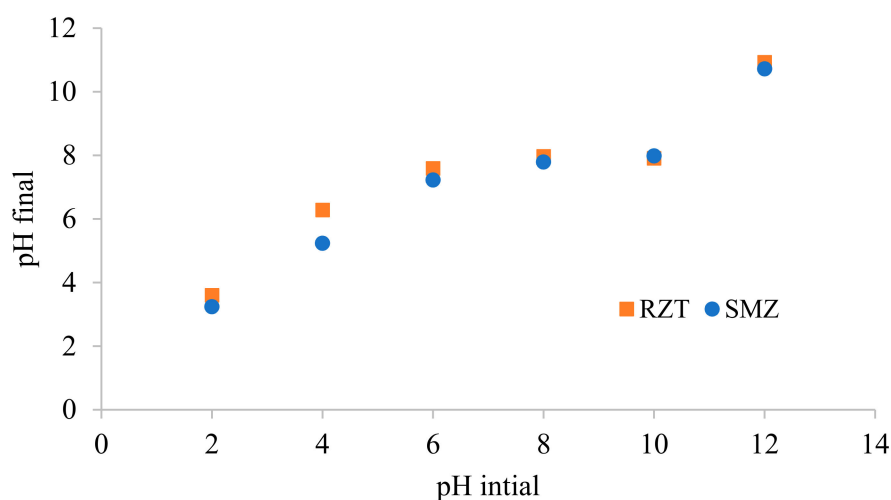


Figure 1. Point zero net charge for raw zeolitic tuff (RZT) and surfactant modified zeolite (SMZ).

Further increasing, $\text{pH}_i > 10.0$ caused an increase in the pH_f . It can be noticed from Figure 1, the trend for the two curves (RZT, SMZ) are similar. The plateaus of each curve mean that for initial pH from 8.0 to 10.0 for RZT and SMZ the addition of the H^+ or OH^- does not influence the equilibrium pH and equal to point of zero charges. Therefore, the pH_{pzc} was determined to be approximately 7.9 for RZT and SMZ. A similar trend was reported by Kragović et al. 2019 for natural zeolite and Fe(III) modified zeolite [28].

According to these results, the pH values of spiked CBZ solutions 6.9–7.2 (Ultrapure) and 7.8–8.2 (WWTP effluent) will relatively have a similar impact on the surface charge of RZT & SMZ.

3.2. X-ray Diffraction

The crystalline structure of RZT and SMZ was characterized using XRD and the results are presented in Figure 2. The XRD pattern of the RZT contains mainly zeolitic phases classified as Phillipsite-Ca faujasite [$\text{Na}_2\text{Al}_2\text{Si}_4\text{O}_{12}\cdot 8\text{H}_2\text{O}$], anorthite [$\text{CaAl}_2\text{Si}_2\text{O}_8$], diopside [$\text{CaMg}(\text{SiO}_3)_2$], and calcite [CaCO_3]. It is well known that phillipsite, faujasite, diopside, calcite, and anorthite are common mineral components that appear in Jordanian zeolitic tuff [19].

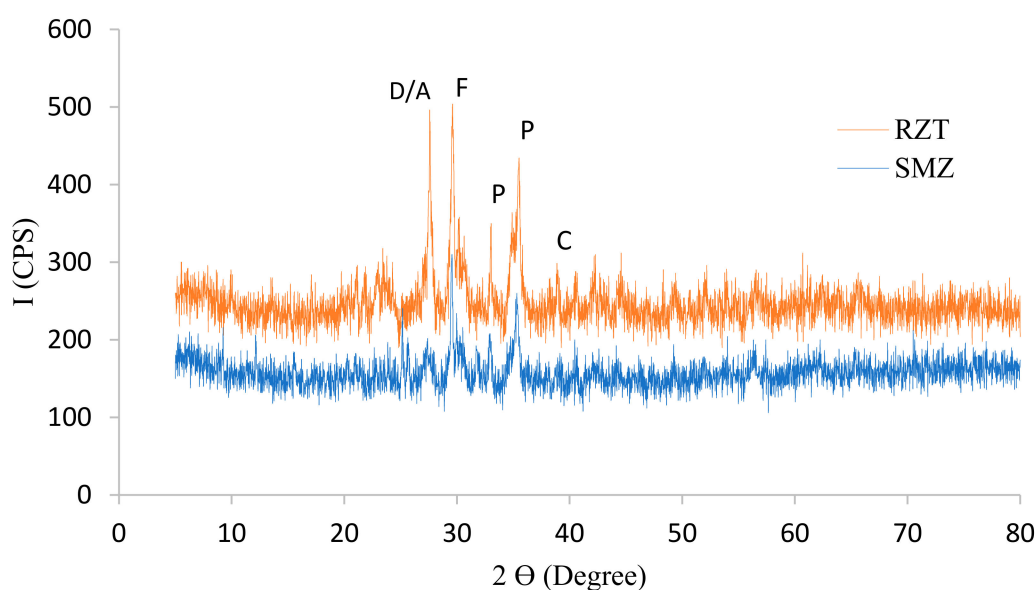


Figure 2. XRD patterns for RZT and SMZ where P—phillipsite, F—Faujasite; A—anorthite, D—diopside; C—calcite.

The XRD results show that the structure of RZT was converted from crystalline to amorphous as well as the intensity of the main peaks disappeared and/or decreased due to the modification of RZT using HDTMA-Br. It is very clear that the crystalline anorthite, diopside, phases disappeared in the SMZ, and the intensity of peaks of crystalline phases such as phillipsite, faujasite, and calcite were considerably decreased.

3.3. X-ray Fluorescence

Table 2 shows the result of XRF analysis for RZT and SMZ. The Si/Al ratio of 3.24, 3.06 were calculated for RZT and SMZ respectively. The major metal oxides present in the sample are SiO_2 , Al_2O_3 , Fe_2O_3 , MgO , CaO , K_2O , and Na_2O . The LOI, which stands for loss on ignition, is considered a common method for determining the organic and carbonate content of samples [31]. The LOI shows the volatile portion after the heating of RZT and SMZ. The loss on ignition percentage of 4.4% and 5.6% for RZT and SMZ, respectively.

3.4. FTIR Spectroscopy

The structure of the RZT and SMZ were investigated using FTIR spectroscopy (Figure 3). There are two strong vibration bands, the first one is in the region of $900\text{--}1200\text{ cm}^{-1}$ and the second one is in the region of $420\text{--}500\text{ cm}^{-1}$, these bands are due to the Si–O–Si and Si–O–Al vibrations. These vibration bands are found in all zeolites because of the internal tetrahedron vibrations and are assigned to a T–O (T = Si or Al) stretching mode and a T–O bending mode for $900\text{--}1200\text{ cm}^{-1}$, $420\text{--}500\text{ cm}^{-1}$ respectively. The peak at 1030 cm^{-1} is unique to phillipsite [32]. At large wavenumber, the results show a similar pattern observed for RZT and SMZ. The band at $\sim 3700\text{ cm}^{-1}$ could be characteristic of H bonded associated

hydroxyl groups of Si(O–H)Al and AlO–H species, at $\sim 3600\text{ cm}^{-1}$ and $\sim 3400\text{ cm}^{-1}$ are considered stretching bands (H–O–H), the adsorbed water molecules on the surface is considered bending band (H–O–H) at 1630 cm^{-1} . The FTIR characterization confirmed the presence of the surfactant molecules on the structure of raw zeolitic tuff. New peaks in SMZ occur at 2920 cm^{-1} and 2850 cm^{-1} and those peaks may result from the alkyl groups of HDTMA on the RZT surface during the modification, also the peaks are attributed to symmetric and asymmetric stretching vibrations of C–C in the alkyl chain and their intensities are reflections of the HDTMA loading [22,27]. It is suggested that the benzene ring and the alkyl groups at CBZ play a major role in CBZ sorption, which further supported the electrostatic interaction between CBZ and positively charged SMZ surfaces. A similar change was reported by Sun et al. 2017 for sorption of diclofenac on zeolite in the presence of cationic surfactant [22].

Table 2. Result of XRF analysis for RZT and SMZ.

Formula	RZT (%)	SMZ (%)
SiO ₂	40.2	42.2
Al ₂ O ₃	12.4	13.8
Fe ₂ O ₃	12.8	14.4
MgO	8.9	9.8
CaO	9.8	10.7
K ₂ O	1.4	1.0
Na ₂ O	1.9	3.3
LOI	4.4	5.6

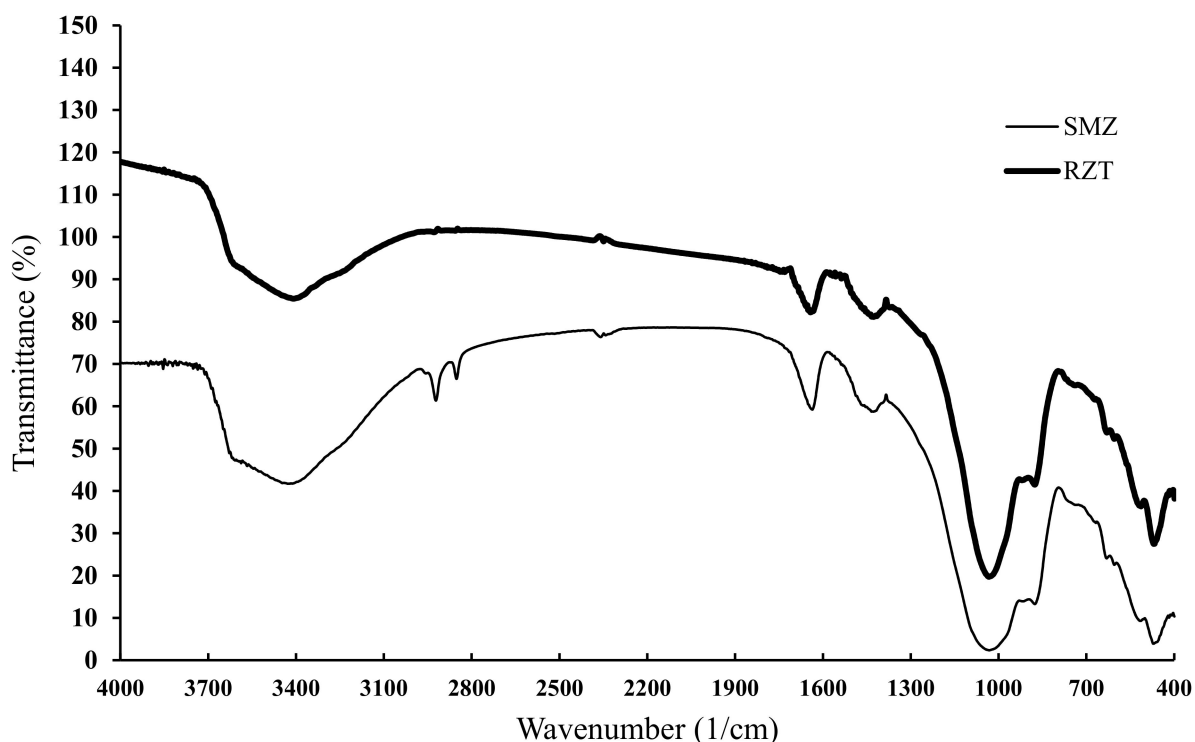


Figure 3. FTIR spectroscopy for the structure of the RZT and SMZ.

3.5. Effect of pH on CBZ Removal

It is well documented that pH is an important factor determining the adsorption capacity in aqueous solutions. The effect of pH on the CBZ adsorption capacity on RZT and SMZ was obtained in the pH value of 2–9.5 (Figure 4).

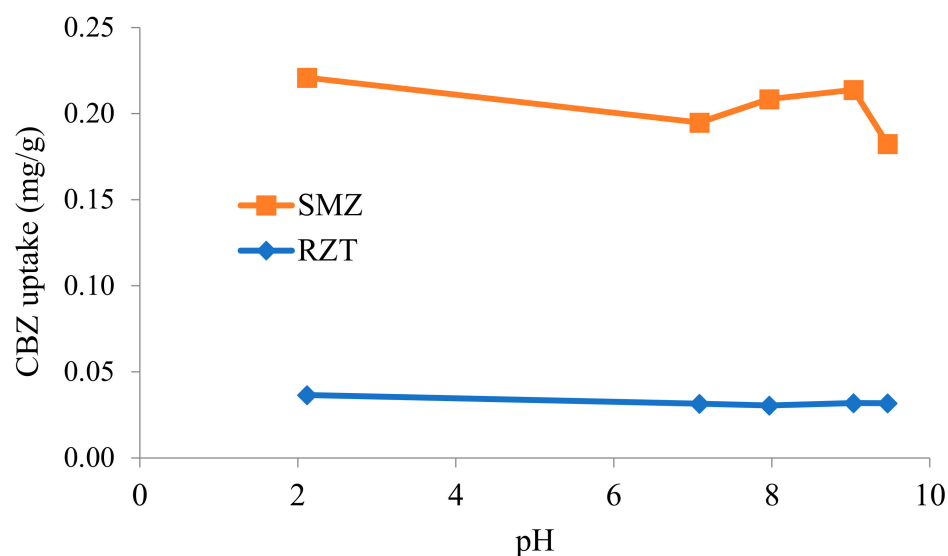


Figure 4. The effect of pH on the carbamazepine (CBZ) adsorption capacity for RZT and SMZ.

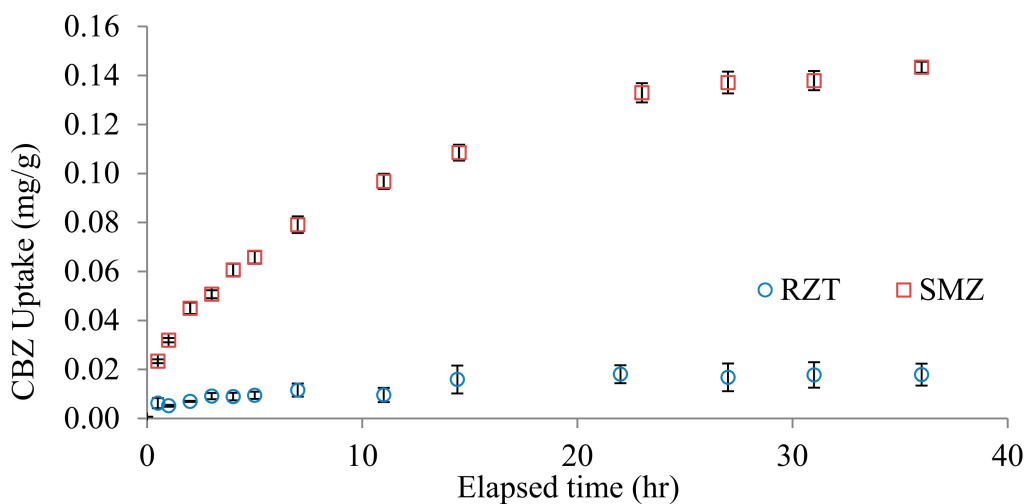
The pKa values of CBZ are 2.3 and 13.9 which suggests a high stability of CBZ in strong acid or alkali solution [33]. As shown in Figure 4 the adsorption of CBZ on RZT is nearly constant (0.03 mg/g) and slight changes for SMZ vary between 7.0 and 9.5 (14% change in uptake). This suggests that RZT and SMZ can be used to remove CBZ from water over a wide pH range. However, the adsorption capacity of CBZ by SMZ is much higher than the RZT and is likely the result of cationic surfactant (HDTMA-Br) on the SMZ surface. FTIR differences suggest that new functional groups on the SMZ surface improve CBZ sorption and are likely due to electrostatic interactions between functional groups of CBZ and positive charge of SMZ. A similar result was reported by Cabrera-Lafaurie et al. 2014 [12]. This study has reported that for the adsorption of CBZ by a synthetic zeolite, no significant changes in uptake amounts were observed upon variation of pH. Jemutai-Kimosopa et al., 2020 showed that CBZ adsorption onto iron oxide modified diatomaceous earth was practically unaffected by pH variation with percent removal ranging between 87.2 and 88.8% in the pH range [13].

3.6. Kinetics Batch Sorption

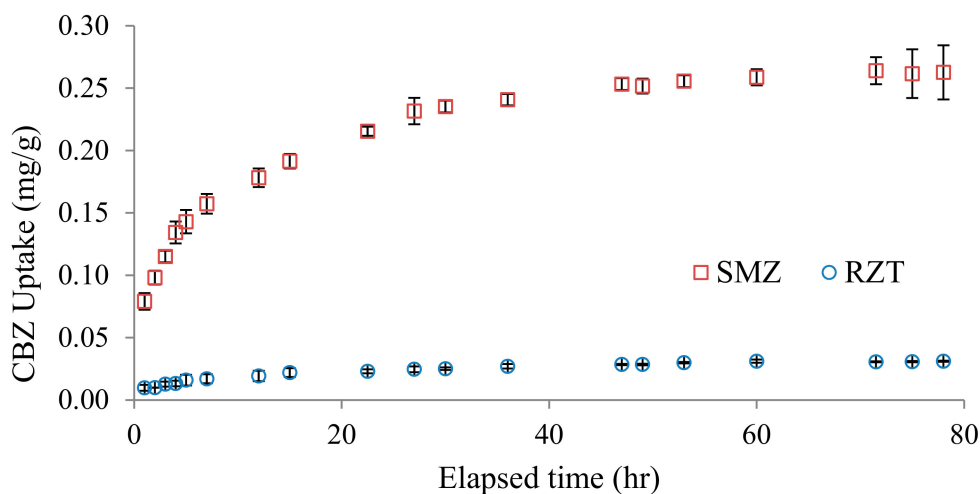
The sorption kinetics results show that the sorption of CBZ was initially rapid followed by a slower process in both the RZT and SMZ using ultrapure water and realistic wastewater matrix (As-Samra wastewater treatment plant effluent) (Figure 5a,b). The error bars are plotted for all collected samples, which shows higher standard deviation values for RZT (0.0002–0.0057) than SMZ (0.0008–0.0044) for CBZ sorption using ultrapure water, while the standard deviation values for RZT (0.0001–0.0043) are lower than SMZ (0.0036–0.0217) at WWTP effluent.

The rate of CBZ uptake decreased with time for RZT and SMZ and the final mass of CBZ adsorbed are clearly different at equilibrium. CBZ sorption uptake shows a different trend between RZT and SMZ. In ultrapure water, the RZT reached a pseudo-equilibrium with uptake (0.018 mg/g) at 22-h, whereas the SMZ reached the equilibrium with uptake (0.14 mg/g) at 27-h. In the case of WWTP effluent, the RZT particles reached a pseudo-equilibrium with uptake (0.029 mg/g) at 47-h, whereas the SMZ reached the equilibrium with uptake (0.25 mg/g) at 47-h. The results showed that the sorption uptake of CBZ increased from 0.018 mg/g (RZT) to 0.14 mg/g (SMZ) in ultrapure water, and from 0.029 mg/g (RZT) to 0.25 mg/g (SMZ) in WWTP effluent. These results suggest that surfactant modification of zeolite has increased the CBZ uptake by 8 and 9-fold for ultrapure water and WWTP effluent respectively. Moreover, these results indicate that the CBZ uptake and its equilibrium time for RZT and SMZ are higher in WWTP effluent than the ultrapure water. The increase in CBZ uptakes are 1.6 and 1.8-fold for RZT and SMZ,

respectively. This is suggesting that the sorption mechanism of CBZ is clearly impacted by the matrix effect. The equilibrium time (22–47 h) of CBZ removal in all batch tests is higher than those reported in the literature (1–4 h). This is mainly due to the large particle size used in this study ($2.36\text{ mm} < \text{selected size} < 4.75\text{ mm}$) compared with the fine particles ($< 200\text{ }\mu\text{m}$) which is usually used in other studies [33].



(a) Ultrapure water

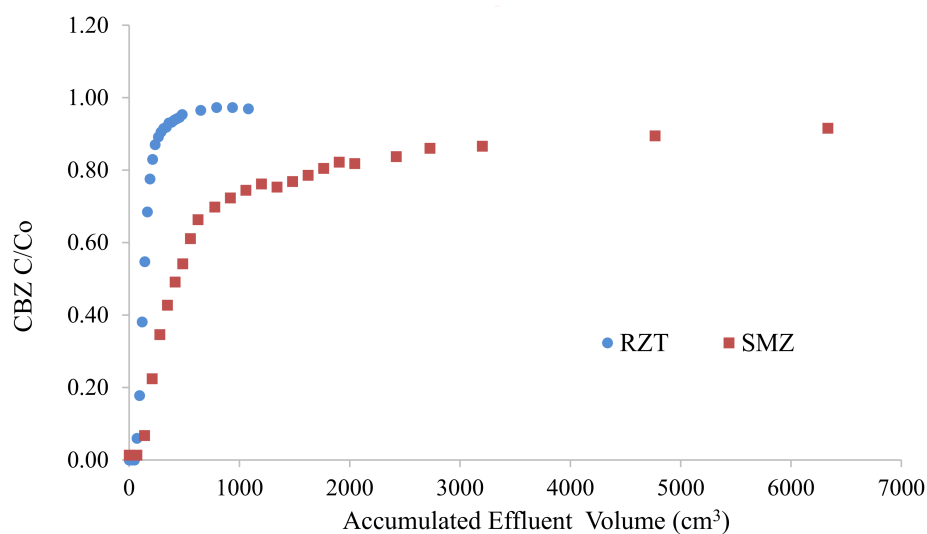


(b) wastewater treatment plant (WWTP) effluent

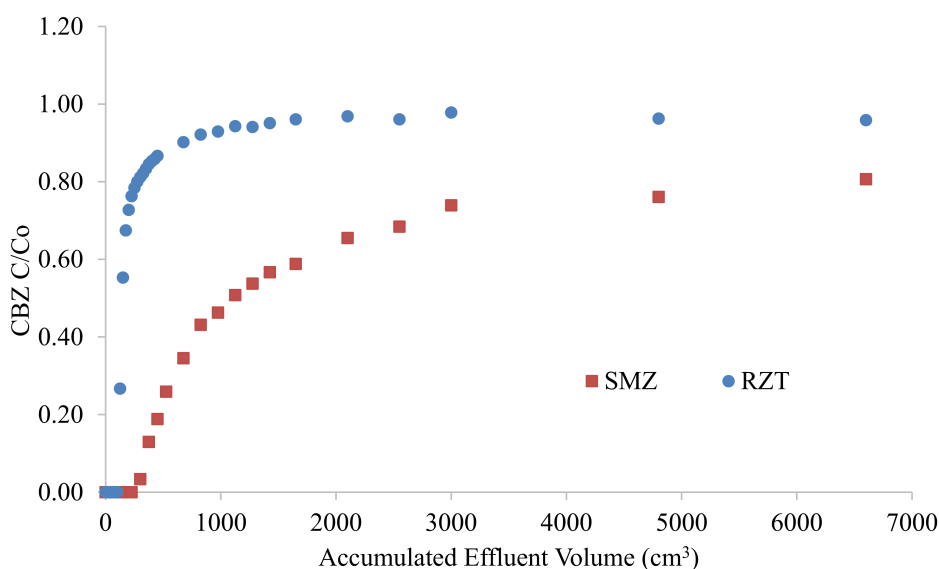
Figure 5. The kinetics of CBZ uptake by RZT and SMZ using (a) ultrapure water and (b) WWTP effluent.

3.7. Column Adsorption

The sustained performance of a filtration-based treatment system for removing dissolved contaminants was evaluated through the use of column tests and breakthrough curves. The breakthrough curves (BTC) for sorption of CBZ onto the RZT and SMZ from $C/C_0 = 0$ to ~ 1 using ultrapure water and WWTP effluent are shown in Figure 6a,b. The BTC for CBZ in the RZT column showed a sharp front with a sigmoidal (S-shaped) breakthrough curve, however the BTC of the SMZ column exhibit slight tailing.



(a) Ultrapure water



(b) WWTP effluent

Figure 6. Breakthrough curves (BTC) for sorption of CBZ onto (a) Ultrapure water (b) WWTP effluent.

In ultrapure water, breakthrough ($C/C_0 = 0.2$) for the RZT column occurs at 94 cm^3 while in the SMZ column it is delayed until 208 cm^3 . This suggests the performance of the RZT column, in terms of time until the breakpoint is reached, is lower than the SMZ column. The sorbed amount of CBZ was calculated by the Simpson rule for RZT and SMZ at $C/C_0 = 0.92$. The results showed that the sorption uptake of CBZ increased from 0.02 mg/g (RZT column) to 0.17 mg/g (SMZ column) by 8.5-fold, which is slightly similar to those achieved in batch tests (8-fold). In WWTP effluent, the breakpoint ($C/C_0 = 0.2$) for the RZT column occurs at 125 cm^3 while in the SMZ column it is delayed until 450 cm^3 . This suggests the performance of the RZT column, in terms of time till the breakpoint is reached, is lower than the SMZ column using ultrapure water and WWTP effluent. The sorbed amount of CBZ was calculated by the Simpson rule for RZT and SMZ at $C/C_0 = 0.93$. The results showed that the sorption uptake of CBZ increased from 0.03 mg/g (RZT column) to 0.33 mg/g (SMZ column) by 11-fold, which is slightly higher than those achieved in batch tests (9-fold). Moreover, the CBZ uptake by RZT and SMZ is higher in WWTP effluent

than the ultrapure water. The increases in CBZ uptake are 1.5 and 2-fold for RZT and SMZ respectively. The positive impact of matrix effect resulted from WWTP effluent on CBZ removal in column test is consistent with those resulted in the batch test (between 1.6 and 1.8-fold).

In summary, the batch and column results indicated that the CBZ uptake by SMZ is higher than RZT using both water matrices. The CBZ uptake by RZT and SMZ in WWTP effluent is higher than in ultrapure water for batch (1.6–1.8 fold) and column test (1.5–2 fold). These findings are suggesting that adsorption of CBZ is positively impacted by the matrix effect. Actually, the matrix of wastewater is completely different from ultrapure water and synthetic wastewater. Wastewater is a complex mixture of a broad range of organic (e.g., humic substances and fulvic acids, carbohydrates, proteins, biopolymers, and building blocks) and inorganic compounds (e.g., carbonate, bicarbonate, nitrite, sulfate, chloride) [26,34]. It has been reported in the literature that the presence of dissolved organic matter (DOM) in wastewater effluents is playing an important role in the adsorption of organic micropollutants onto activated carbon [24,25]. Moreover, contrasting impacts have been observed in experimental studies because of the influence of co-existing DOM [24–26]. The positive impact of organic background on CBZ adsorption by RZT and SMZ in this study is consistent with some previous studies. For example, Wang et al. showed that the sorption of A polychlorinated biphenyls on biochars was greatly enhanced in the presence of organic matter (humic acid, HA) [35]. This phenomenon was explained that when HA was sorbed to the surface of biochar, it could also provide more sorption sites for PCBs [35]. On the other hand, a negative impact of existing DOM on micropollutant adsorption using activated carbon due to competition effects on the material surface [25]. In conclusion, the role of DOM in the adsorption of micropollutants varied significantly, depending on adsorption conditions. Therefore, further investigations are required to explain the interaction of DOM with the adsorption mechanism of CBZ under realistic wastewater conditions.

4. Conclusions

Adsorption of CBZ was significantly achieved by surface modification using batch and column experiments in different water matrices. The pH_{pzc} was determined to be approximately 7.9 for RZT and SMZ. XRD showed the modification of RZT by HDTMA-Br created an amorphous surface. Furthermore, FTIR confirmed the modification of RZT had created alkyl groups on the surface of the SMZ. This suggested that electrostatic interactions between functional groups of CBZ and the positive charge of SMZ have increased the sorption. In general, surfactant modification of RZT has increased the CBZ uptake using batch and column tests. The CBZ uptake by RZT and SMZ in WWTP effluent is higher than ultrapure water for batch and column tests. This is might be due to the presence of DOM in the wastewater matrix. It is expected that the outcomes of this study will give insight into CBZ removal by SMZ from realistic wastewater and provide the basis for further development of zeolite modification and enhanced its application in wastewater treatment systems.

Author Contributions: The idea for the study was developed by O.A.A.-M. and S.L.B.-H. O.A.A.-M. supervised and administrated the project. The design of the experiment method was provided by O.A.A.-M., S.L.B.-H. and D.D.S. L.Z.A. carried out instrument analysis. Formal analysis, data curation, writing the paper and manuscript review were accomplished by O.A.A.-M., D.A.A., L.Z.A., S.L.B.-H. and D.D.S. All authors have read and agreed to the published version of the manuscript.

Funding: This research was supported by the Partnership for Enhanced Engagement in Research (PEER) program administered by the National Academy of Sciences (NAS) and funded by the United States Agency for International Development (USAID), Project number: 5-91 (Cycle 5) “The occurrence and fate of pharmaceutical residues from their sources to water bodies and food chain”.

Acknowledgments: The study was supported by the Partnership for Enhanced Engagement in Research (PEER) program administered by the National Academy of Sciences (NAS) and funded by

the United States Agency for International Development (USAID), Project number: 5-91 (Cycle 5) “The occurrence and fate of pharmaceutical residues from their sources to water bodies and food chain”. We would like to thank Robert McLaughlan for the constructive comments for the result analysis and discussion.

Conflicts of Interest: The authors declare no conflict of interest.

References

- Zhang, Y.; Geißen, S.-U.; Gal, C. Carbamazepine and diclofenac: Removal in wastewater treatment plants and occurrence in water bodies. *Chemosphere* **2008**, *73*, 1151–1161. [[CrossRef](#)]
- Bui, T.X.; Choi, H. Influence of ionic strength, anions, cations, and natural organic matter on the adsorption of pharmaceuticals to silica. *Chemosphere* **2010**, *80*, 681–686. [[CrossRef](#)]
- Papageorgiou, M.; Kosma, C.; Lambropoulou, D. Seasonal occurrence, removal, mass loading and environmental risk assessment of 55 pharmaceuticals and personal care products in a municipal wastewater treatment plant in Central Greece. *Sci. Total. Environ.* **2016**, *543*, 547–569. [[CrossRef](#)]
- Balakrishna, K.; Rath, A.; Praveenkumarreddy, Y.; Guruge, K.S.; Subedi, B. A review of the occurrence of pharmaceuticals and personal care products in Indian water bodies. *Ecotoxicol. Environ. Saf.* **2017**, *137*, 113–120. [[CrossRef](#)] [[PubMed](#)]
- Nguyen, H.T.; Thai, P.K.; Kaserzon, S.L.; O’Brien, J.W.; Eaglesham, G.; Mueller, J.F. Assessment of drugs and personal care products biomarkers in the influent and effluent of two wastewater treatment plants in Ho Chi Minh City, Vietnam. *Sci. Total. Environ.* **2018**, *631–632*, 469–475. [[CrossRef](#)]
- Al-Mashaqbeh, O.; Alsafadi, D.; Dalahmeh, S.; Bartelt-Hunt, S.; Snow, D. Snow Removal of Selected Pharmaceuticals and Personal Care Products in Wastewater Treatment Plant in Jordan. *Water* **2019**, *11*, 2004. [[CrossRef](#)]
- Thacker, P.D. Pharmaceutical Data Elude Researchers. *Environ. sci. technol.* **2005**, *39*, 193a–194a. [[PubMed](#)]
- Dvory, N.Z.; Kuznetsov, M.; Livshitz, Y.; Gasser, G.; Pankratov, I.; Lev, O.; Adar, E.; Yakirevich, A. Modeling sewage leakage and transport in carbonate aquifer using carbamazepine as an indicator. *Water Res.* **2018**, *128*, 157–170. [[CrossRef](#)]
- Thomas, M.A.; Klaper, R.D. Psychoactive Pharmaceuticals Induce Fish Gene Expression Profiles Associated with Human Idiopathic Autism. *PLoS ONE* **2012**, *7*, e32917. [[CrossRef](#)] [[PubMed](#)]
- Dávila-Estrada, M.; Ramírez-García, J.J.; Díaz-Nava, M.C.; Solache-Ríos, M. Sorption of 17 α -Ethinylestradiol by Surfactant-Modified Zeolite-Rich Tuff from Aqueous Solutions. *Water Air Soil Pollut.* **2016**, *227*, 157. [[CrossRef](#)]
- Dávila-Estrada, M.; Ramírez-García, J.J.; Solache-Ríos, M.J.; Gallegos-Pérez, J.L. Kinetic and Equilibrium Sorption Studies of Ceftriaxone and Paracetamol by Surfactant-Modified Zeolite. *Water Air Soil Pollut.* **2018**, *229*, 123. [[CrossRef](#)]
- Cabrera-Lafaurie, W.A.; Román, F.R.; Hernández-Maldonado, A.J. Removal of salicylic acid and carbamazepine from aqueous solution with Y-zeolites modified with extraframework transition metal and surfactant cations: Equilibrium and fixed-bed adsorption. *J. Environ. Chem. Eng.* **2014**, *2*, 899–906. [[CrossRef](#)]
- Jemutai-Kimosop, S.; Orata, F.; Shikuku, V.O.; Okello, V.A.; Getenga, Z.M. Insights on adsorption of carbamazepine onto iron oxide modified diatomaceous earth: Kinetics, isotherms, thermodynamics, and mechanisms. *Environ. Res.* **2020**, *180*, 108898. [[CrossRef](#)]
- Wang, S.; Peng, Y. Natural zeolites as effective adsorbents in water and wastewater treatment. *Chem. Eng. J.* **2010**, *156*, 11–24. [[CrossRef](#)]
- Alkaram, U.F.; Mukhlis, A.A.; Al-Dujaili, A.H. The removal of phenol from aqueous solutions by adsorption using surfactant-modified bentonite and kaolinite. *J. Hazard. Mater.* **2009**, *169*, 324–332. [[CrossRef](#)] [[PubMed](#)]
- Xie, J.; Meng, W.; Wu, D.; Zhang, Z.; Kong, H. Removal of organic pollutants by surfactant modified zeolite: Comparison between ionizable phenolic compounds and non-ionizable organic compounds. *J. Hazard. Mater.* **2012**, *231–232*, 57–63.
- Catrinescu, C.; Apreutesei, R.E.; Teodosiu, C. Surfactant-modified natural zeolites for environmental applications in water purification. *Environ. Eng. Manag. J.* **2008**, *7*, 149–161. [[CrossRef](#)]
- De Gennaro, B.; Catalanotti, L.; Bowman, R.S.; Mercurio, M. Anion exchange selectivity of surfactant modified clinoptilolite-rich tuff for environmental remediation. *J. Colloid Interface Sci.* **2014**, *430*, 178–183. [[CrossRef](#)] [[PubMed](#)]
- Al-Jammal, N.; Juzsakova, T.; Zsirka, B.; Sebestyén, V.; Németh, J.; Cretescu, I.; Halmágyi, T.; Domokos, E.; Rédey, Á. Modified Jordanian zeolitic tuff in hydrocarbon removal from surface water. *J. Environ. Manag.* **2019**, *239*, 333–341. [[CrossRef](#)] [[PubMed](#)]
- Hashemi, M.S.H.; Eslami, F.; Karimzadeh, R. Organic contaminants removal from industrial wastewater by CTAB treated synthetic zeolite Y. *J. Environ. Manag.* **2019**, *233*, 785–792. [[CrossRef](#)]
- Nodehi, R.; Shayesteh, H.; Kelishami, A.R. Enhanced adsorption of congo red using cationic surfactant functionalized zeolite particles. *Microchem. J.* **2020**, *153*, 104281. [[CrossRef](#)]
- Sun, K.; Shi, Y.; Wang, X.; Li, Z. Sorption and retention of diclofenac on zeolite in the presence of cationic surfactant. *J. Hazard. Mater.* **2017**, *323*, 584–592. [[CrossRef](#)]
- Gagliano, E.; Sgroi, M.; Falciglia, P.P.; Vagliasindi, F.G.; Roccaro, P. Removal of poly- and perfluoroalkyl substances (PFAS) from water by adsorption: Role of PFAS chain length, effect of organic matter and challenges in adsorbent regeneration. *Water Res.* **2020**, *171*, 115381. [[CrossRef](#)] [[PubMed](#)]

24. De Ridder, D.J.; Verliefde, A.R.D.; Heijman, S.G.J.; Verberk, J.Q.J.C.; Rietveld, L.C.; Van Der Aa, L.T.J.; Amy, G.L.; Van Dijk, J.C. Influence of natural organic matter on equilibrium adsorption of neutral and charged pharmaceuticals onto activated carbon. *Water Sci. Technol.* **2011**, *63*, 416–423. [[CrossRef](#)] [[PubMed](#)]
25. Mailler, R.; Gasperi, J.; Coquet, Y.; Derome, C.; Buleté, A.; Vulliet, E.; Bressy, A.; Varrault, G.; Chebbo, G.; Rocher, V. Removal of emerging micropollutants from wastewater by activated carbon adsorption: Experimental study of different activated carbons and factors influencing the adsorption of micropollutants in wastewater. *J. Environ. Chem. Eng.* **2016**, *4*, 1102–1109. [[CrossRef](#)]
26. Haddad, M.; Oie, C.; Duy, S.V.; Sauvé, S.; Barbeau, B. Adsorption of micropollutants present in surface waters onto polymeric resins: Impact of resin type and water matrix on performance. *Sci. Total. Environ.* **2019**, *660*, 1449–1458. [[CrossRef](#)]
27. Smiljanić, D.; de Gennaro, B.; Izzo, F.; Langella, A.; Daković, A.; Germinario, C.; Rottinghaus, G.E.; Spasojević, M.; Mercurio, M. Removal of emerging contaminants from water by zeolite-rich composites: A first approach aiming at diclofenac and ketoprofen. *Microporous Mesoporous Mater.* **2020**, *298*, 110057. [[CrossRef](#)]
28. Kragović, M.; Stojmenović, M.; Petrović, J.; Loredo, J.; Pašalić, S.; Nedeljković, A.; Ristović, I. Influence of Alginate Encapsulation on Point of Zero Charge (pHpzc) and Thermodynamic Properties of the Natural and Fe(III) - Modified Zeolite. *Procedia Manuf.* **2019**, *32*, 286–293. [[CrossRef](#)]
29. Tom, D.; Reynolds, P.R. *Unit Operations and Processes in Environmental Engineering*; PWS Publishing Co.: Boston, MA, USA, 1996.
30. Gulicovski, J.J.; Čerović, L.S.; Milonjić, S.K. Point of Zero Charge and Isoelectric Point of Alumina. *Mater. Manuf. Process.* **2008**, *23*, 615–619. [[CrossRef](#)]
31. Heiri, O.; Lotter, A.F.; Lemcke, G. Loss on ignition as a method for estimating organic and carbonate content in sediments: Reproducibility and comparability of results. *J. Paleolimnol.* **2001**, *25*, 101–110. [[CrossRef](#)]
32. To, M.-H.; Hadi, P.; Hui, C.-W.; Lin, C.S.K.; McKay, G. Mechanistic study of atenolol, acebutolol and carbamazepine adsorption on waste biomass derived activated carbon. *J. Mol. Liq.* **2017**, *241*, 386–398. [[CrossRef](#)]
33. Al-Jammal, N.; Al-Hamamre, Z.; Alnaief, M. Manufacturing of zeolite based catalyst from zeolite tuft for biodiesel production from waste sunflower oil. *Renew. Energy* **2016**, *93*, 449–459. [[CrossRef](#)]
34. Ribeiro, A.R.L.; Moreira, N.F.; Puma, G.L.; Silva, A.M. Impact of water matrix on the removal of micropollutants by advanced oxidation technologies. *Chem. Eng. J.* **2019**, *363*, 155–173. [[CrossRef](#)]
35. Wang, Y.; Wang, L.; Fang, G.; Herath, H.; Wang, Y.; Cang, L.; Xie, Z.; Zhou, D. Enhanced PCBs sorption on biochars as affected by environmental factors: Humic acid and metal cations. *Environ. Pollut.* **2013**, *172*, 86–93. [[CrossRef](#)] [[PubMed](#)]